DCT quantization matrices visually optimized for individual images

Andrew Watson

Andrew B. Watson, "DCT quantization matrices visually optimized for individual images," Proc. SPIE 1913, Human Vision, Visual Processing, and Digital Display IV, (8 September 1993); doi: 10.1117/12.152694

SPIE.

Event: IS&T/SPIE's Symposium on Electronic Imaging: Science and Technology, 1993, San Jose, CA, United States

DCT quantization matrices visually optimized for individual images

Andrew B. Watson

MS 262-2 NASA Ames Research Center
Moffett Field, CA 94035-1000
beau@vision.arc.nasa.gov

ABSTRACT

Several image compression standards (JPEG, MPEG, H.261) are based on the Discrete Cosine Transform (DCT). These standards do not specify the actual DCT quantization matrix. Ahumada & Peterson[1] and Peterson, Ahumada & Watson[2] provide mathematical formulae to compute a perceptually lossless quantization matrix. Here I show how to compute a matrix that is optimized for a particular image. The method treats each DCT coefficient as an approximation to the local response of a visual "channel." For a given quantization matrix, the DCT quantization errors are adjusted by contrast sensitivity, light adaptation, and contrast masking, and are pooled non-linearly over the blocks of the image. This yields an 8x8 "perceptual error matrix." A second non-linear pooling over the perceptual error matrix yields total perceptual error. With this model we may estimate the quantization matrix for a particular image that yields minimum bit rate for a given total perceptual error, or minimum perceptual error for a given bit rate. Custom matrices for a number of images show clear improvement over image-independent matrices. Custom matrices are compatible with the JPEG standard, which requires transmission of the quantization matrix.

1. JPEG DCT QUANTIZATION

The JPEG image compression standard provides a mechanism by which images may be compressed and shared among users [3, 4]. I briefly review the quantization process within this standard. The image is first divided into blocks of size {8,8}. Each block is transformed into its DCT, which we write c_{ijk}, where i,j indexes the DCT frequency (or basis function), and k indexes a block of the image. Though the blocks themselves form a two dimensional array, for present purposes a one dimensional block index is sufficient. Each block is then quantized by dividing it, coefficient by coefficient, by a quantization matrix (QM) q_{ij}, and rounding to the nearest integer

$$u_{ijk} = \text{Round}\left[c_{ijk}/q_{ij}\right] \quad . \tag{1}$$

The quantization error e_{ijk} in the DCT domain is then

$$e_{ijk} = c_{ijk} - u_{ijk}\, q_{ij} \quad . \tag{2}$$

2. IMAGE-INDEPENDENT PERCEPTUAL QUANTIZATION

The JPEG QM is not defined by the standard, but is supplied by the user and stored or transmitted with the compressed image. The principle that should guide the design of a JPEG QM is that it provide optimum visual quality for a given bit rate. QM design thus depends upon the visibility of quantization errors at the various DCT frequencies. In recent papers, Peterson *et al.* [5, 6] have provided measurements of threshold amplitudes for DCT basis functions. For each frequency ij they measured psychophysically the smallest coefficient that yielded a visible signal. Call this threshold t_{ij}. From Eqn.s (1) and (2) it is clear that the maximum possible quantization error e_{ijk} is $q_{ij}/2$. Thus to ensure that all errors are invisible (below threshold), we set

$$q_{ij} = 2\, t_{ij} \quad . \tag{3}$$

 0-8194-1146-9/93/$6.00

I call this the Image-Independent Perceptual approach (IIP). It is perceptual because it depends explicitly upon detection thresholds for DCT basis functions, but is image-independent because a single matrix is computed independent of any image. Ahumada *et al.* [1,7] have extended the value of this approach by measuring t_{ij} under various conditions and by providing a formula that allows extrapolation to other display luminances (L) and pixel sizes (px,py), as well as other display properties. For future reference, we write this formula in symbolic form as

$$t_{ij} = \mathrm{ap}[i, j, L, px, py, \ldots] \tag{4}$$

3. LIMITATIONS OF THE IIP APPROACH

While a great advance over the *ad hoc* matrices that preceded it, the IIP approach has several shortcomings. The fundamental drawback is that the matrix is computed independent of the image. This would not be a problem if visual thresholds for artifacts were fixed and independent of the image upon which they are superimposed, but this is not the case.

First, visual thresholds increase with background luminance. The formula of Ahumada & Peterson describes the threshold for DCT basis functions as a function of a mean luminance. This would normally be taken as the mean luminance of the display. But variations in local mean luminance within the image will in fact produce substantial variations in DCT threshold. We call this *luminance masking*.

Second, threshold for a visual pattern is typically reduced in the presence of other patterns, particularly those of similar spatial frequency and orientation, a phenomenon usually called *contrast masking*. This means that threshold error in a particular DCT coefficient in a particular block of the image will be a function of the value of that coefficient in the original image.

Third, the IIP approach ensures that any single error is below threshold. But in a typical image there are many errors, of varying magnitudes. The visibility of this error ensemble is not generally equal to the visibility of the largest error, but reflects a pooling of errors, over both frequencies and blocks of the image. I call this *error pooling*.

Fourth, when all errors are kept below a perceptual threshold a certain bit rate will result. The IIP method gives no guidance on what to do when a lower bit rate is desired. The ad hoc "quality factors" employed in some JPEG implementations, which usually do no more than multiply the quantization matrix by a scalar, will allow an arbitrary bit rate, but do not guarantee (or even suggest) optimum quality at that bit rate. I call this the problem of *selectable quality.*

Here I present a general method of designing a custom quantization matrix tailored to a particular image. This *image-dependent perceptual* (IDP) method incorporates solutions to each of the problems described above: luminance masking, contrast masking, error pooling, and selectable quality. The strategy is to develop a very simple model of perceptual error, based upon DCT coefficients, and to iteratively estimate the quantization matrix which yields a designated perceptual error.

4. LUMINANCE MASKING

Detection threshold for a luminance pattern typically depends upon the mean luminance of the local image region: the brighter the background, the higher the luminance threshold [8,9]. This is usually called "light adaptation," but here we call it "luminance masking" to emphasize the similarity to contrast masking, discussed in the next section.

To illustrate this effect, the solid lines in Fig. 1 plot values of the formula for t_{ij} provided by Ahumada and Peterson[1] as a function of the mean luminance of the block, assuming that the maximum display luminance is 100 cd m^{-2} and that the greyscale resolution is 8 bits. The three curves are for five representative frequencies. These

curves illustrate that variations by as much as 0.5 log unit in t_{ij} might be expected to occur within an image, due to variations in the mean luminance of the block.

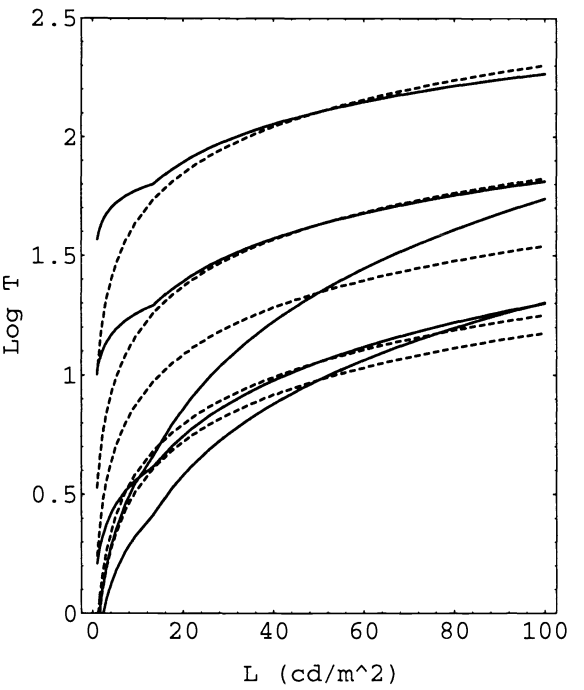

Figure 1. Log of t_{ij} as a function of luminance L of the block. From the top, the curves are for frequencies of {7,7}, {0,7}, {0,0}, {0,3}, and {0,1}. The maximum display luminance is assumed to be 100 cd m^{-2}. The dashed curves are the power function approximation described in the text.

The effect of mean luminance upon the DCT thresholds is complex, involving both vertical and horizontal shifts of the contrast sensitivity function. We can compute a luminance-masked threshold matrix for each block in either of two ways. The first is to make use of a formula such as that supplied by Ahumada and Peterson [1],

$$t_{ijk} = \mathrm{ap}[i, j, L_0\, c_{00k}/\bar{c}_{00}] \tag{5}$$

where c_{00k} is the DC coefficient of the DCT for block k., L_0 is the mean luminance of the display, and $\bar{c}_{00}$ is the DC coefficient corresponding to L_0 (1024 for an 8 bit image). This solution is as complete and accurate as the underlying formula, but may be rather expensive to compute. For example, in the *Mathematica* language, using a compiled function, and running on a SUN Sparc 2, it takes about 1 second per block.

A second, simpler solution is to approximate the dependence of t_{ij} upon c_{00k} with a power function:

$$t_{ijk} = t_{ij}\left(c_{00k}/\bar{c}_{00}\right)^{a_T} \quad . \tag{6}$$

The initial calculation of t_{ij} should be made assuming a display luminance of L_0 The parameter a_T takes its name from the corresponding parameter in the formula of Ahumada and Peterson, wherein they suggest a value of 0.649. Note that luminance masking may be suppressed by setting a_T=0. More generally, a_T controls the degree to which this masking occurs. Note also that the power function makes it easy to incorporate a non-unity display Gamma, by multiplying a_T by the Gamma exponent (see Section 10.2).

As illustrated by the dashed lines in Fig. 1, this power function approximation is accurate over an upper range of luminances (for the parameters in Fig. 1, above about 10 cd m^{-2}). Except for very dark sections of an image, this range should be adequate. The discrepancy is also greatest at the lowest frequencies, especially the DC term. This could be corrected by adopting a matrix of exponents, one for each frequency. But note that the discrepancy is a conservative one, that is the threshold changes less with block luminance than the model calls for. This may not be a bad thing, especially at DC, where the validity of the model may be least.

5. CONTRAST MASKING

Contrast masking refers to the reduction in the visibility of one image component by the presence of another. This masking is strongest when both components are of the same spatial frequency, orientation, and location. Here we consider only masking within a block and a particular DCT coefficient (It is possible to extend these ideas to masking between DCT coefficients, and across DCT blocks). We employ a model of visual masking that has been widely used in vision models, based on seminal work by Legge and Foley [10, 11]. Given a DCT coefficient c_{ijk} and a corresponding absolute threshold t_{ijk} our masking rule states that the masked threshold m_{ijk} will be

$$m_{ijk} = \mathrm{Max}\left[t_{ijk} \, , \, \left|c_{ijk}\right|^{w_{ij}} t_{ijk}^{\,1-w_{ij}} \right] \tag{7}$$

where w_{ij} is an exponent that lies between 0 and 1. Because the exponent may differ for each frequency, we allow a matrix of exponents equal in size to the DCT. Note that when w_{ij} =0, no masking occurs, and the threshold is constant at t_{ijk}. When w_{ij} = 1, we have what is usually called "Weber Law" behavior, and threshold is constant in log or percentage terms (for $c_{ijk} > t_{ijk}$). The function is pictured for a typical empirical value of w_{ij} = 0.7 in Fig. 2.

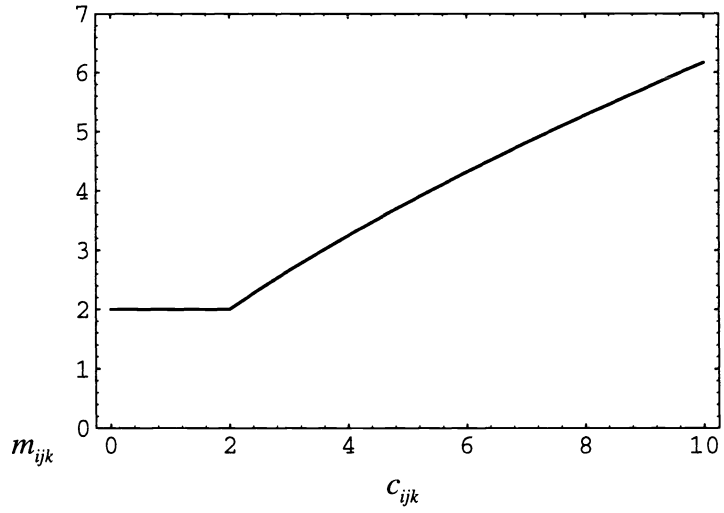

Figure 2. Contrast masking function, describing the masked threshold m_{ijk} as a function of DCT coefficient c_{ijk} , for parameters w_{ij}=0.7, t_{ijk} = 2.

Because the effect of the DC coefficient upon thresholds has already been expressed by luminance masking, we specifically exclude the DC term from the contrast masking, by setting the value of $w_{00} = 0$. It is interesting that while contrast masking is assumed to be independent from coefficient to coefficient (frequency to frequency), in the case of luminance masking the DC frequency affects *all* other frequencies.

Figure 3 shows the masked sensitivity (m_{ijk}^{-1}) for the Lena image. Note that the dark strip in the upper right results in generally higher sensitivity due to luminance masking (un-masking, perhaps we should say).

Figure 3. The Lena image and its masked sensitivity DCT (m_{ijk}^{-1}) for w_{ij}=0.7 and a_T=0.649. If w_{ij}=0 and a_T=0, all cells would be identical and would look like the inset (2 t_{ij}).

6. PERCEPTUAL ERROR AND JUST-NOTICEABLE-DIFFERENCES

In vision science, we often express the magnitude of a signal in multiples of the threshold for that signal. These threshold units are often called "just-noticeable differences," or *jnd*'s. Having computed a masked threshold m_{ijk}, the error DCT may therefore be expressed in jnd's as

$$d_{ijk} = e_{ijk} / m_{ijk} \tag{8}$$

Each value of d_{ijk} is an error in a particular frequency and block, expressed as a proportion of the just-detectable error in that frequency and block. Thus all the errors are now in the "common coin" of perceptual error, the *jnd*.

7. SPATIAL ERROR POOLING

To pool the errors in the jnd DCT we employ another standard feature of current vision models: the so-called β-norm (or Minkowski metric). It often arises from an attempt to combine the separate probabilities that individual errors will be seen, in the scheme known as "probability summation" [12, 13, 14]. We pool the jnds for a particular frequency {*i,j*} over all blocks *k* as

$$p_{ij} = \left(\sum_k \left| d_{ijk} \right|^{\beta_s} \right)^{1/\beta_s} \tag{9}$$

Different values of the exponent β_s implement different types or degrees of pooling. When β_s=1, the pooling is linear summation of absolute values. When β_s=2, the errors combine quadratically, in an RMS or standard deviation type measure. When $\beta_s = \infty$(in practice, a large number such as 100 will do), the pooling rule becomes a maximum-of operation: only the largest error matters. In psychophysical experiments that examine

summation among sinusoidal components of differing frequency, a β_s of about 4 has been observed [15, 16, 17]. The exponent β_s is given here as a scalar, but may be made a matrix equal in size to the QM to allow differing pooling behavior for different DCT frequencies. This matrix p_{ij} of "pooled jnds" is now a simple measure of the visibility of artifacts within each of the frequency bands defined by the DCT basis functions. I call it the "perceptual error matrix."

8. FREQUENCY ERROR POOLING

This perceptual error matrix p_{ij} may itself be of value in revealing the frequencies that result in the greatest pooled error for a particular image and quantization matrix. But to optimize the matrix we would like a single-valued perceptual error metric. We obtain this by combining the elements in the perceptual error matrix, using a Minkowski metric with a possibly different exponent , β_f

$$P = \left(\sum_{ij} p_{ij}^{\beta_f} \right)^{1/\beta_f} . \tag{10}$$

It is now straightforward, at least conceptually, to optimize the quantization matrix to obtain minimum bit-rate for a given P, or minimum P for a given bit rate. In practice, however, a solution may be difficult to compute. But if $\beta_f = \infty$, then P is given by the maximum of the p_{ij}. Under this condition minimum bit-rate for a given $P = \psi$ is achieved when all $p_{ij} = \psi$. Intuitively, if the maximum of the p_{ij} equals ψ, each of the others might as well be increased to ψ, since that will not increase P, but will decrease bit-rate.

Recall that each entry in the matrix p_{ij} corresponds (at least monotonically) with the visibility of a particular class of artifact: that of the corresponding frequency (basis function). This strategy of equating all p_{ij} to ψ thus also has the effect of equating the visibilities of each of these classes of error.

While it is likely that the true value of β_f is nearer to β_s (approximately 4), it also seems likely that this more accurate value will not greatly alter the outcome of the optimization and will not be worth the substantial increase in computational effort.

8. OPTIMIZATION METHOD

Under the assumption $\beta_f = \infty$, the joint optimization of the quantization matrix reduces to the vastly simpler separate optimization of the individual elements of the matrix. Each entry of the perceptual error matrix p_{ij} may be considered an independent function of the corresponding entry q_{ij} of the quantization matrix

$$p_{ij} = \mathrm{f}_{ij}\left(q_{ij}\right) . \tag{11}$$

This function is monotonically increasing and

$$f_{ij}(1) = 0 \quad \forall \ i, j . \tag{12}$$

We seek a particular $\hat{q}_{ij}$ such that

$$f_{ij}\left(\hat{q}_{ij}\right) = \psi \quad \forall \ i, j . \tag{13}$$

Of course, in some cases no amount of quantization will yield a value as large as the target ψ (for example, if all coefficients are quantized to 0, but the error remains below ψ). For those cases we are content to set $\hat{q}_{ij}$ to an arbitrary maximum, such as 255 (the largest quantization table entry permitted in the JPEG baseline standard).

In a practical implementation, a rapid method of estimating $\hat{q}_{ij}$ is required. Here we have used a bisection method that, while slow, is guaranteed to find a solution. A range is established for q_{ij} between lower and upper bounds of $\overset{<}{q}_{ij}$ and $\overset{>}{q}_{ij}$ (typically {1,255}). p_{ij} is evaluated at the midpoint of the range,

$$\overline{q}_{ij} = \text{Round}\left[\frac{1}{2}\left(\overset{<}{q}_{ij} + \overset{>}{q}_{ij}\right)\right] . \tag{14}$$

If $p_{ij} < \psi$, then $\overset{<}{q}_{ij} = \overline{q}_{ij}$, otherwise, $\overset{>}{q}_{ij} = \overline{q}_{ij}$. This procedure is repeated until $\overline{q}_{ij}$ no longer changes. As a practical matter, since QM's in baseline JPEG are eight bit integers, this degree of accuracy is obtained in n=9 iterations from a starting range of 255 .

In the following examples, unless otherwise stated, the parameter values used were $a_T = 0.649$, $\beta = 4$, $w_{ij} = 0.7$, display mean luminance $L_0 = 65$ cd m^{-2} , image greylevels = 256, $\overline{c}_{00} = 1024$. The viewing distance was assumed to yeild 32 pixels/degree. For a 256 by 256 pixel image, this corresponds to a viewing distance if 7.115 picture heights. The "JPEG bit rate" is calculated by computing the code size for AC and DC coefficients using the default JPEG Huffman tables. It does not include the overhead composed of quantization tables, Huffman tables, marker codes, etc. because this overhead is not image dependent and depends on coding decisions made by the application (e.g. use of restart intervals). If it had been included it would increase the bit rate for a 256 by 256 image by about 0.038 bits/pixel.

Several steps in the iterative estimation of $\hat{q}_{ij}$ are illustrated in Fig. 4. Successive steps show further refinement in $\hat{q}_{ij}$, and a progressively more uniform matrix p_{ij}. On step 1, $q_{ij} = 255$, $\forall \; i,j$. On this step the perceptual error matrix shows greatest error at low spatial frequencies.

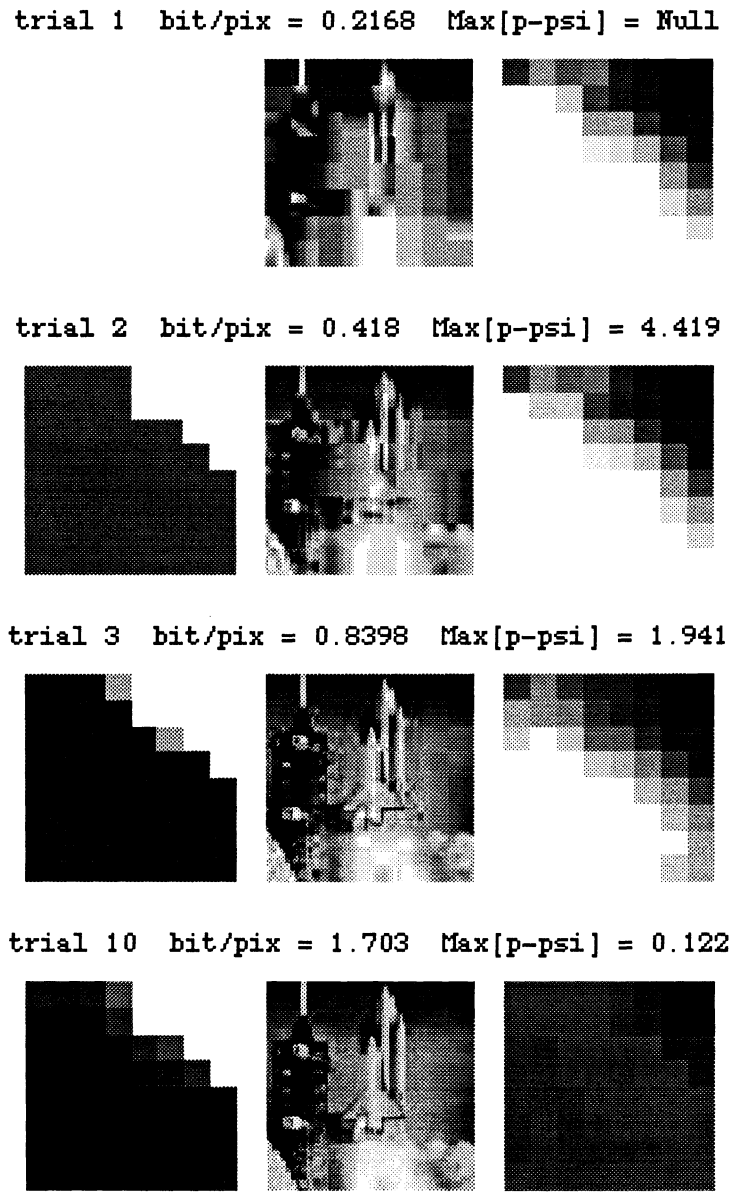

Figure 4. Iterative estimation of the custom quantization matrix $\hat{q}_{ij}$. The three panels in each row show quantization matrix q_{ij}, the reconstructed image using q_{ij}, and the perceptual error matrix p_{ij}. The labels indicate the iteration trial, the current JPEG bit-rate, and the maximum difference between p_{ij} and ψ (discounting those for which the maximum error is always less than ψ). The image was {64,64}, target ψ was 1. For q_{ij} and p_{ij}, the DC coefficient is at the lower left corner.

Figure 5 shows the Lena image [18] compressed to various values of perceptual error ψ = {1, 2, 4, 8}. The value of ψ=1 produces an essentially "perceptually lossless" compression [19] under the prescribed viewing conditions (mean luminance = 65 cd m^{-2}, 32 pixels/deg.

Figure 5. The Lena image compressed using custom matrices designed for perceptual error levels (ψ) of 1, 2, 4, and 8. Corresponding bit rates were 2.28, 1.47, 0.72, 0.24. The original image had dimensions of {256,256}.

It is interesting to compare the image-independent quantization matrix to the custom matrix for various quality levels. This is shown in Table 1, where we give the ratio of image-dependent and independent matrices, for two quality levels of 1 and 4. Elements that have been set to the maximum of 255 are indicated by zeros. Note that image dependence does alter the structure of the matrix, and that changes in quality (as defined here) do not yield a constant scaling of the basic matrix.

0.156	0.231	0.193	0.208	0.192	0.165	0.172	0.161
0.231	0.223	0.208	0.179	0.182	0.167	0.146	0.155
0.193	0.208	0.166	0.174	0.171	0.157	0.156	0.171
0.162	0.179	0.174	0.165	0.154	0.158	0.166	0.194
0.157	0.141	0.171	0.154	0.156	0.166	0.164	0.243
0.165	0.167	0.157	0.158	0.195	0.208	0.226	0.289
0.172	0.168	0.156	0.181	0.198	0.235	0.317	
0.187	0.171	0.158	0.217	0.251			

0.615	1.41	1.24	1.13	1.07	1.46	
1.1	1.11	1.28	1.04	1.15	1.38	3.28
1.07	1.1	1.11	1.22	1.28	1.55	
1.04	1.1	1.26	1.25	1.72		
1.55	1.39	1.69	2.05			

Table 1. Ratio of image-dependent and independent quantization matrices for the Lena image at quality levels of 1 (top) and 4 (bottom). This ratio is equal to $\hat{q}_{ij}/2t_{ij}$. Empty cells indicate that the image-dependent matrix had a value of 255 (the maximum allowed).

9. OPTIMIZING QM FOR A GIVEN BIT-RATE

It is of interest to relate the JPEG bit-rate to the perceptual error level ψ. This is shown for the Lena and Mandrill images in Fig. 6. This is a sort of inverse "rate-distortion" function. Note that useful bit-rates below 2 bits/pixel yield perceptual errors above about 2.

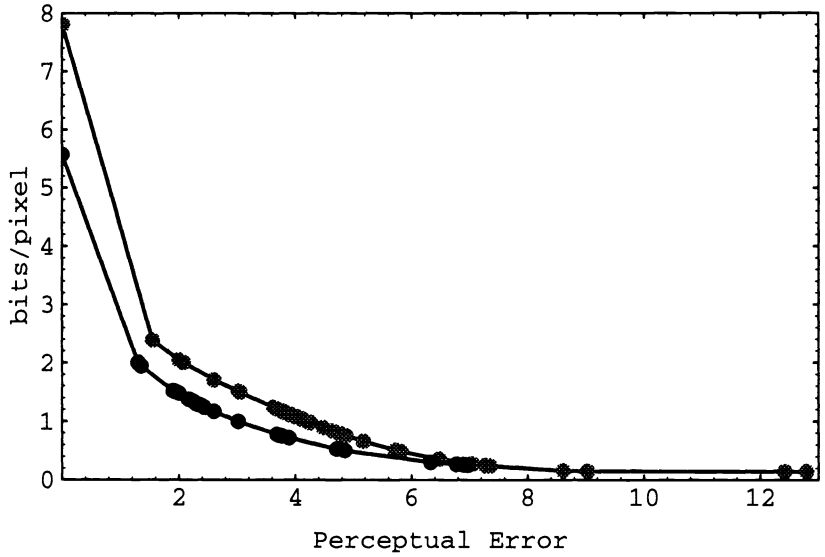

Figure 6. JPEG bit-rate versus perceptual error ψ for the Lena (lower curve) and Mandrill (upper curve) images. The lines are second order polynomial interpolations.

The method described above yields a QM with a specified perceptual error ψ. However, one may desire a QM that yields a given bit rate h_0 with minimum perceptual error ψ. This can be done iteratively by noting that the bit rate is a decreasing function of ψ, as shown in Fig. 6. In our current implementation, we use a second order interpolating polynomial fit to all previous estimated values of $\{h, \psi\}$ to estimate the next candidate ψ, terminating when $|h - h_0| < \Delta h$, where Δh is the desired accuracy in bit-rate. On each iteration, a complete estimation of $\hat{q}_{ij}$ is performed. There are no doubt more rapid methods.

The most meaningful contest between IDP and IIP approaches is to compare images compressed by the two methods to a constant bit rate. Furthermore, the bit rate must be low enough that the poorer method shows visible artifacts, else both will appear perfect. Figures 7 and 8 provide such comparisons. The IDP method is visibly superior, even in relatively low-quality printed renditions.

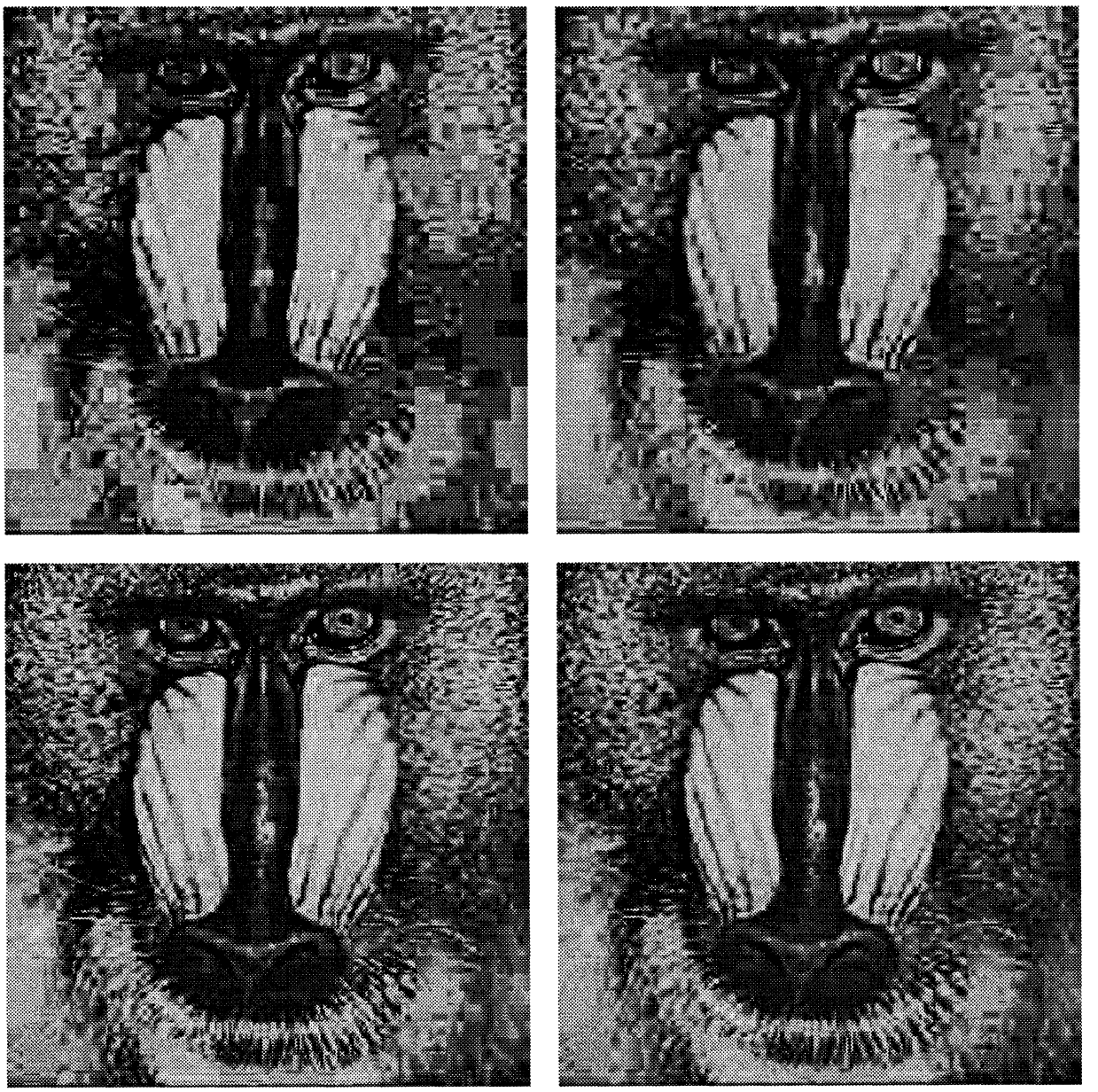

Figure 7. IIP (left) and IDP (right) compressions at 0.25 bits/pixel (top row) and 0.5 bits/pixel (bottom row).

Figure 8. IIP (left) and IDP (right) compressions at 0.25 bits/pixel (top row) and 0.5 bits/pixel (bottom row).

10. EXTENSIONS AND FUTURE RESEARCH

10.1 Estimation of t_{ij} w_{ij}, β_s, a_T

The method described here depends upon estimates of the matrices t_{ij} and w_{ij}, and the parameters β_s and a_T. Estimates of t_{ij} may be obtained directly from psychophysical experiments that measure detection thresholds for individual DCT basis functions [1, 5, 6]. We are devising experiments, adapted from the methods of Legge and Foley [10, 11] to directly estimate w_{ij}. In these experiments detection thresholds are measured for an increment (or

decrement) in the amplitude of a DCT basis function. Estimation of β_s is more difficult. Several values of β_s in the range of 1-100 could be evaluated for the degree to which they yield a plausible perceptual error metric p_{ij}. In addition, a matrix of values of β_s might be warranted, with different degrees of spatial pooling at each DCT frequency.

10.2 Gamma Functions

Remarkably, the JPEG specification makes no statement regarding the relation between pixel values and displayed luminance. While one can understand their reluctance to impose constraints upon JPEG applications, it should be understood that ultimate visual quality depend on this relation. The "de facto" assumption appears to be that pixel values will be applied directly to the display subsystem, which typically has a non-linear relation between greylevel and luminance, often known as a "gamma function" that is approximately a power function with an exponent (gamma) of about 2.3. The assumption presumably also is that variations in this function from system to system are not so great as to seriously degrade visual quality.

In an ideal system, one would specify both the gamma function of image capture, and of the target display. Image data would be transformed to luminance before compression, and after reconstruction, to values that would result in luminance on the display. Unfortunately, we cannot add descriptors of these gamma functions to the existing JPEG specification, so we must be content with the "de facto" assumption.

Since the preceding calculations have treated pixel values as proportional to luminance (gamma=1), under the "de facto" assumption, we should subject the image data to inverse and forward gamma transformations before coding and after decoding, respectively. The present approach, which does no such transformations, relies on the approximate linearity of the gamma function near the middle of its range, and on the inclusion of the display gamma into the luminance masking function as discussed in Section 4. This subject will be examined in future research.

10.3 Color Images

The Image-Dependent Perceptual approach has been described here only with respect to coding of monochrome images. The principles, however, are easily extended to color images. The simplest approach is to measure or compute a unique t_{ij} for each of the three color channels[7], and from them compute three custom quantization matrices. The matter may be complicated by different masking and pooling properties in the chromatic channels than in the luminance channel. But since color consumes so small a part of the total bit-rate, these details are not likely to be critical in practical applications.

11. SUMMARY

I have shown how to compute a visually optimal quantization matrix for a given image. These image-dependent quantization matrices produce better results than image independent matrices. The algorithm can be easily incorporated into JPEG compliant applications.

In a practical sense, the IDP method proposed here solves two problems. The first is to provide maximum visual quality for a given bit rate. The second problem it solves is to provide the user with a sensible and meaningful quality scale for JPEG compression. Without such a scale, each image must be repeatedly compressed, reconstructed, and evaluated by eye to find the desired level of visual quality.

However, at present, it is admittedly only a conjecture that this scale relates in a direct way to perceived visual quality. While I am confident that it relates more directly to quality than does the ad hoc "quality factor" of some JPEG implementations, to demonstrate a robust relation between computed perceptual error and perceived quality will require subjective judgments, both over different bit rates and different images.

From the standpoint of computational complexity, this algorithm adds only a modest amount to the cost of JPEG image compression. All optimization takes place in the DCT domain, so no additional forward or inverse DCT's are required. The DCT mask is computed only once, and consists of a few calculations on each DCT pixel. The estimation of the quantization matrix requires a maximum of ten (and probably many fewer) iterations, each of which consists of a modest number of simple operations on each DCT pixel. It is certainly a smaller burden than requiring the user to repeatedly compress, reconstruct, and visually assess the result.

12. NOTATION

c_{ijk}	DCT of an image
q_{ij}	quantization matrix
u_{ijk}	quantized DCT
e_{ijk}	DCT error
t_{ij}	DCT threshold matrix (based on global mean luminance)
$\mathrm{ap}[i,j,L,px,py,\ldots]$	threshold formula of Ahumada and Peterson[1]
t_{ijk}	DCT threshold matrix (based on local mean luminance c_{00k})
a_T	luminance masking exponent
w_{ij}	contrast masking exponent (Weber exponent)
m_{ijk}	mask DCT
d_{ijk}	jnd DCT
p_{ij}	perceptual error matrix
β_s	spatial error-pooling exponent
P	total perceptual error
β_f	frequency error-pooling exponent
c_{00k}	DC coefficient in block k
L_0	mean luminance of the display
$\bar{c}_{00}$	Average DC coefficient, corresponding to L_0 (typically 1024)
Ψ	target total perceptual error value
$\hat{q}_{ij}$	estimated quantization matrix yielding target perceptual error

13. ACKNOWLEDGMENTS

I thank Albert J. Ahumada, Jr. and Heidi A. Peterson for valuable discussions. This work was supported by NASA RTOPs 506-59-65 and 505-64-53.

14. REFERENCES

1. A. J. Ahumada Jr. and H. A. Peterson. "Luminance-Model-Based DCT Quantization for Color Image Compression," in *Human Vision, Visual Processing, and Digital Display III*, B. E. Rogowitz, ed. (Proceedings of the SPIE, 1992).

2. H. A. Peterson, A. J. Ahumada Jr. and A. B. Watson. "The Visibility of DCT Quantization Noise," SID Digest of Technical Papers, in press (1993).

3. G. Wallace. "The JPEG still picture compression standard," Communications of the ACM. **34**(4), 30-44 (1991).

4. W. B. Pennebaker and J. L. Mitchell. *JPEG Still image data compression standard* (Van Nostrand Reinhold, New York, 1993).

5. H. A. Peterson. "DCT basis function visibility in RGB space," in *Society for Information Display Digest of Technical Papers*, J. Morreale, ed. (Society for Information Display, Playa del Rey, CA, 1992).

6. H. A. Peterson, H. Peng, J. H. Morgan and W. B. Pennebaker. "Quantization of color image components in the DCT domain,". Human Vision, Visual Processing, and Digital Display. Proc. SPIE. **1453**: 210-222, 1991.

7. H. A. Peterson, A. J. Ahumada Jr. and A. B. Watson. "An improved detection model for DCT coefficient quantization," SPIE Proceedings. **1913** (In press), (1993).

8. F. L. van Nes and M. A. Bouman. "Spatial modulation transfer in the human eye," Journal of the Optical Society of America. **57**, 401-406 (1967).

9. H. B. Barlow. "Dark and light adaptation: Psychophysics," in *Handbook of Sensory Physiology*, L. Hurvich and D. Jameson, ed. (Springer-Verlag, New York, 1972).

10. G. E. Legge and J. M. Foley. "Contrast masking in human vision," Journal of the Optical Society of America. **70**(12), 1458-1471 (1980).

11. G. E. Legge. "A power law for contrast discrimination," Vision Research. **21**, 457-467 (1981).

12. N. Graham. "Visual detection of aperiodic spatial stimuli by probability summation among narrowband detectors," Vision Research. **17** , 37-652 (1977).

13. J. G. Robson and N. Graham. "Probability summation and regional variation in contrast sensitivity across the visual field," Vision Research. **21**, 409-418 (1981).

14. A. B. Watson. "Probability summation over time," Vision Research. **19**, 515-522 (1979).

15. N. Graham and J. Nachmias. "Detection of grating patterns containing two spatial frequencies: a comparison of single-channel and multiple-channel models," Vision Research. **11**, 251-259 (1971).

16. N. Graham, J. G. Robson and J. Nachmias. "Grating summation in fovea and periphery," Vision Research. **18**, 815-825 (1978).

17. A. B. Watson and J. Nachmias. "Summation of asynchronous gratings," Vision Research. **20** , 91-94 (1980).

18. A. Weber. *Image data base (USCIPI Report 1070)* (Image Processing Institute, University of Southern California, Los Angeles, CA, 1983).

19. A. B. Watson. "Receptive fields and visual representations," SPIE Proceedings. **1077**, 190-197 (1989).